Image Processing by Topological Asymptotic Expansion

Didier Auroux · Mohamed Masmoudi

Abstract The aim of this article is to recall the applications of the topological asymptotic expansion to major image processing problems. We briefly review the topological asymptotic analysis, and then present its historical application to the crack localization problem from boundary measurements. A very natural application of this technique in image processing is the inpainting problem, which can be solved by identifying the optimal localization of the missing edges. A second natural application is then the image restoration or enhancement. The identification of the main edges of the image allows us to preserve them, and smooth the image outside the edges. If the conductivity outside edges goes to infinity, the regularized image is piecewise constant and provides a natural solution to the segmentation problem. The numerical results presented for each application are very promising. Finally, we must mention that all these problems are solved with a $\mathcal{O}(n \cdot \log(n))$ complexity.

Keywords Topological asymptotic expansion ·
Topological gradient · Edge detection · Image inpainting ·
Image restoration · Image segmentation

1 Introduction

The goal of topological optimization and most image processing problems is to create a partition of a given domain (or set) Ω of $\mathbb{R}^2$:

D. Auroux (✉) · M. Masmoudi
Institut de Mathématiques de Toulouse, Université Paul Sabatier
Toulouse 3, 31062 Toulouse cedex 9, France
e-mail: auroux@mip.ups-tlse.fr

- In topological optimization, we look for the optimal design $\omega \subset \Omega$ and its complementary;
- In image processing problems like edge detection, classification, and segmentation, the goal is to split the image in several parts.

For this reason, topological shape optimization and image processing problems have common mathematical methods like level set approaches, material properties optimization, variational methods, ... In this paper, we will only consider the topological gradient approach that has been introduced for topological optimization purpose [7, 8, 36–38, 44, 50, 54, 57].

To find the optimal domain ω is equivalent to identify its characteristic function $\mathcal{X}_\omega$. At first sight this problem is not differentiable. The classical ways to make it differentiable are [3–6, 20, 21, 56, 59]:

- The relaxation technique, which allows $\mathcal{X}_\omega$ to take all possible values in the interval [0, 1];
- The level set approach where the characteristic function is replaced by a regular level set function which is positive inside ω and negative in its complementary.

The topological asymptotic expansion gives the variation of a cost function when we switch $\mathcal{X}_\omega$ from one to zero or from zero to one in a small area.

In this paper we focus our interest on the application of the topological asymptotic expansion approach to edge detection, which is the basis of our image processing algorithms. We will consider the classical thermal diffusion technique [28, 49, 52, 60, 61] and improve it by modelling the edges by cracks. These cracks are supposed to be highly insolating and allow to the temperature to jump across edges.

More precisely, let Ω be an open bounded domain of $\mathbb{R}^2$. In our context edges are modeled by cracks. A crack

$\sigma(x, n, \rho)$ is a straight line of length 2ρ, centered at the point x of Ω, and normal to the unit vector n. For a small $\rho \geq 0$, let $\Omega_\rho = \Omega \backslash \sigma(x, n, \rho)$ be the perturbed domain by the insertion of a small crack.

Let $j(\Omega) := J(u_\Omega)$ be a cost function to be minimized, where u_Ω is the solution to a second order Partial Differential Equations (PDE) problem defined in Ω. The topological sensitivity theory provides an asymptotic expansion of j when ρ tends to zero. It takes the general form

$$j(\Omega_\rho) - j(\Omega) = f(\rho)g(x, n) + \circ(f(\rho)), \qquad (1)$$

where $f(\rho)$ is an explicit positive function going to zero with ρ, $g(x, n)$ is called the topological gradient at point x, and $\circ(f(\rho))$ is a small rest. Then to minimize the criterion j, we have to insert small cracks at points where g is negative. Using this gradient type information, it is possible to build fast algorithms. In most applications, a satisfying approximation of the optimal solution is reached at the first iteration of the optimization process. A topological sensitivity framework allowing to obtain such an expansion for general cost functions has been proposed in [36–38, 44].

The starting point of this work is the inverse conductivity problem, known as the Calderon problem [27]. It consists in identifying the thermal conductivity in a domain from external boundary measurements of temperature when known fluxes are applied. This problem has been widely studied in literature [34, 35, 41, 42]. In the particular case of cracks identification, the problem seems to be more convenient to solve thanks to the singularities of the solution. Only two measurements are needed to recover several simple cracks [1, 2, 8, 17]. From the numerical point of view, several methods [9, 18, 19, 25, 26, 34, 46, 53] have been proposed, but the topological gradient approach seems to be the most efficient method for crack localization [8].

The basic idea of this paper is to adapt this crack localization method to image processing problems: an image can be viewed as a piecewise smooth function and edges can be seen as a set of singularities or cracks. The idea of relaxing continuity constraints through the choice of a non-constant diffusion coefficient is very classical [58], but the topological gradient approach provides an accurate identification of the discontinuities.

As a first and natural application in the image processing field, we consider the inpainting problem. The goal of inpainting is to fill a hidden part of an image. In other words, if we denote by Ω the original image and ω the hidden part of the image, our goal is to recover the hidden part from the known part of the image in $\Omega \backslash \omega$. Here the interior of ω is not empty: it is not a random set nor a narrow line.

This problem has been widely studied and many methods have been considered:

- Learning approaches (neural networks, radial basis functions, support vector machine, . . .); the learning data is taken in $\Omega \backslash \omega$, then the approximate function is evaluated in ω [63, 64];
- Minimization of an energy cost function in ω based on a total variation norm [29, 30];
- Morphological component analysis methods separating texture and cartoon [33].

Crack detection allows to identify the edges of the hidden part of the image, and the inpainting problem is then solved easily.

As a second application of this crack identification technique, we consider the image restoration problem. We recall that a classical way to restore an image u from its noisy version v defined in a domain $\Omega \subset \mathbb{R}^2$ is to solve the following PDE problem

$$\begin{cases} -\operatorname{div}(c\nabla u) + u = v & \text{in } \Omega, \\ \partial_n u = 0 & \text{on } \partial\Omega, \end{cases} \qquad (2)$$

where c is a small positive constant, ∂_n denotes the normal derivative and n is the outward unit normal to $\partial\Omega$, the boundary of Ω. This method is well known to give poor results: it blurs important structures like edges. In order to improve this method, nonlinear isotropic and anisotropic methods were introduced, we can cite here the work of Perona and Malik [49], Catté et al. [28] and more recently Weickert [60, 61] and Aubert [11, 12]. Partial Differential Equations is not the only way to solve the restoration problem, as a representative to statistical methods, we can cite [32].

In topological gradient approach, c takes only two values: c_0 in the smooth part of the image and a small value ε on edges or cracks. For this reason, classical nonlinear diffusive approaches, where c takes all the values of the interval $[\varepsilon, c_0]$, could be seen as a relaxation of our method. By enlarging the set of admissible solutions, relaxation increases the instability of the restoration process and this could explain why our method is so efficient: only one iteration is needed.

This paper is concerned also with the problem of segmentation which it consists in splitting an image into its constituent parts. We first apply the restoration algorithm to find edges. Then, we take a large background conductivity outside edges ($c = c_0/\varepsilon$). If ε goes to infinity, the limit solution u is piecewise constant outside edges and provides a natural segmentation of the image. This approach has been partly studied in the case of medical images [43].

Many approaches have been proposed in literature. We can cite here some variational approaches such as the use of the Mumford-Shah functional [45], or active contours and snakes [23, 55]. We can cite here some commonly used models like the structural approach by regions growth [48], the stochastic approaches [22, 24] and the variational approaches which are based on various strategies like level set formulations, the Mumford-Shah functional, active contours

and geodesic active contours methods or wavelet transforms [10, 11, 13, 45, 47, 51, 52, 62].

This article is organized as follows. In Sect. 2, we recall our method for crack localization using the topological gradient. In Sect. 3, we present the adaptation of this technique to inpainting. Section 4 is devoted to the image restoration problem. In Sect. 5, we couple our restoration algorithm with a segmentation method. We present in Sect. 6 a very efficient way to speed up all the algorithms introduced in this paper. We end the paper with some concluding remarks in Sect. 7.

2 Crack Localization Problem

2.1 Problem Setting

We recall in this section the crack detection technique presented in [8]. Let Ω be a bounded open set of $\mathbb{R}^2$. We assume that there is a perfectly insulating crack σ^* inside the domain. We impose a flux $\phi \in H^{-1/2}(\Gamma)$ on the boundary Γ of Ω, and for a given crack $\sigma \subset \Omega$, we consider the temperature $u \in H^1(\Omega\backslash\sigma)$, solution to

$$\begin{cases} \Delta u = 0 & \text{in } \Omega\backslash\sigma, \\ \partial_n u = \phi & \text{on } \Gamma, \\ \partial_n u = 0 & \text{on } \sigma. \end{cases} \tag{3}$$

In order to have a well-posed direct problem (3), we assume that

$$\int_\Gamma \phi \, ds = 0, \tag{4}$$

and

$$\int_{\Omega\backslash\sigma} u \, dx = 0. \tag{5}$$

Moreover, the solution u to (3) has to satisfy $u_{|\Gamma} = T$ where T is a given function of $H^{1/2}(\Gamma)$. This additional boundary condition could be satisfied by finding optimal distributions of cracks inside the domain Ω.

As we have an over-determination in the boundary conditions, we can define a *Dirichlet* and a *Neumann* problem:

$$\text{Find} \quad u_D \in H^1(\Omega\backslash\sigma) \quad \text{such that} \quad \begin{cases} \Delta u_D = 0 & \text{in } \Omega\backslash\sigma, \\ u_D = T & \text{on } \Gamma, \\ \partial_n u_D = 0 & \text{on } \sigma, \end{cases}$$
$$\tag{6}$$

and

$$\text{find} \quad u_N \in H^1(\Omega\backslash\sigma) \quad \text{such that} \quad \begin{cases} \Delta u_N = 0 & \text{in } \Omega\backslash\sigma, \\ \partial_n u_N = \phi & \text{on } \Gamma, \\ \partial_n u_N = 0 & \text{on } \sigma. \end{cases}$$
$$\tag{7}$$

The normal derivative of the solution is equal to zero on both sides of σ. The gradient of the solution is tangent to the crack if we consider the domain $\Omega\backslash\sigma$, but in the domain Ω the gradient is defined in the distribution sense and is normal to the crack. We are on the edge of the image.

It is clear that for the actual crack σ^*, the two solutions u_D and u_N are equal. The idea is then to consider the following cost function:

$$J(\sigma) = \frac{1}{2}\|u_D - u_N\|^2_{L^2(\Omega)}, \tag{8}$$

where u_D and u_N are solutions to problems (6) and (7) respectively for the given crack σ.

2.2 Localization of Cracks by Topological Asymptotic Analysis

We consider in this section the two corresponding adjoint states, respectively solutions in $H^1(\Omega)$ to

$$\begin{cases} -\Delta p_D = -(u_D - u_N) & \text{in } \Omega, \\ p_D = 0 & \text{on } \Gamma, \end{cases} \tag{9}$$

and

$$\begin{cases} -\Delta p_N = +(u_D - u_N) & \text{in } \Omega, \\ \partial_n p_N = 0 & \text{on } \Gamma. \end{cases} \tag{10}$$

The variation of the cost function $j(\rho) := J(u_{\sigma(x,n,\rho)})$ induced by the insertion of this small crack is given by the topological gradient theory [8]:

$$j(\rho) - j(0) = f(\rho)g(x,n) + o(f(\rho)), \tag{11}$$

where $f(\rho) = \pi\rho^2$ and g is given by

$$g(x,n) = -[(\nabla u_D(x).n)(\nabla p_D(x).n)$$
$$+ (\nabla u_N(x).n)(\nabla p_N(x).n)]. \tag{12}$$

The solutions $u_D, u_N, p_D,$ and p_N are calculated in the initial domain Ω without any crack. The topological gradient can then be rewritten in the following way

$$g(x,n) = n^T M(x)n, \tag{13}$$

where $M(x)$ is the 2×2 symmetric matrix defined by

$$M(x) = -\text{sym}\left(\nabla u_D(x).\nabla p_D(x)^T + \nabla u_N(x).\nabla p_N(x)^T\right).$$
$$\tag{14}$$

We can deduce that $g(x,n)$ is minimal when the normal n is the eigenvector associated to the smallest (i.e. most negative) eigenvalue of the matrix $M(x)$. In the following, this eigenvalue will be considered as the topological gradient.

We can then define a simple and very fast numerical algorithm. First, we solve the two direct problems (Dirichlet

Fig. 1 *Left*: actual cracks; *right*: superposition of the actual cracks and a topological gradient isovalue. Figure extracted from [8]
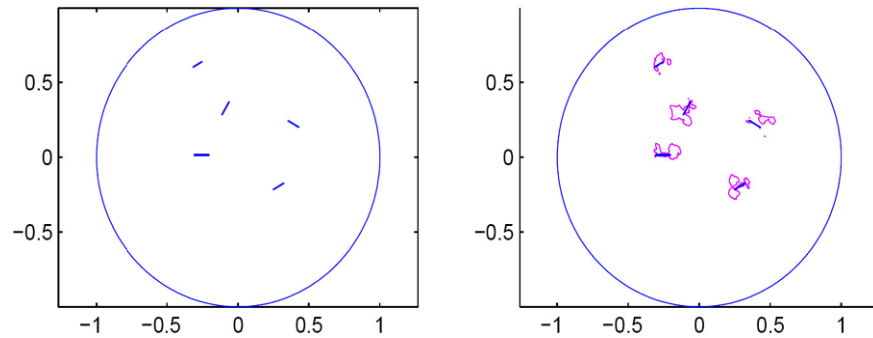
and Neumann), and the two corresponding adjoint problems. Then, at each point x of the domain, we compute the matrix $M(x)$ and its two eigenvalues. The crack likely lies in the most negative gradient regions.

Applying the procedure described above, an example of localization of the unknown cracks using the topological gradient is shown in Fig. 1 (extracted from [8]). The most negative values of the topological gradient are located around the actual cracks, and these results are obtained in only one iteration.

3 Application to Inpainting Problems

Our image inpainting approach is based on the hypothesis that the image is regular outside edges. We suppose even that it is harmonic ($\Delta u = 0$). Of course, this assumption is not valid in real applications, but it gives a theoretical justification of our algorithm, which still works if the image is not harmonic outside edges. The basic idea is then to create a harmonic extension of the image from boundary estimation of u and $\partial_n u$. This analytic extension is unique when it exists. The cracks identification process gives the boundary of the domain of validity of the extension.

3.1 Algorithm

We denote by Ω the image and Γ its boundary, ω the missing part of the image and γ its boundary. In the following v represents the image we want to restore, T will represent here the value of the image on the boundary of the missing zone, and ϕ will be the corresponding flux. We have then $T = v$ and $\phi = \partial_n v$ in the corresponding domains. Theoretically, we have to assume v to be enough regular, for example in $H^2(\Omega)$, but it will be possible to work with v in $L^2(\Omega)$.

We now consider the problem of finding $u_\alpha \in H^1(\Omega)$, solution to the following equation:

$$\begin{cases} -\alpha \Delta u_\alpha + u_\alpha \cdot \chi_{\Omega \setminus \omega} = v \cdot \chi_{\Omega \setminus \omega} & \text{in } \Omega, \\ \partial_n u_\alpha = 0 & \text{on } \Gamma, \end{cases} \quad (15)$$

where α is a small positive number. This equation can be rewritten as

find $u_\alpha \in H^1(\Omega)$

such that $\begin{cases} -\alpha \Delta u_\alpha + u_\alpha = v & \text{in } \Omega \setminus \omega, \\ \Delta u_\alpha = 0 & \text{in } \omega, \\ \partial_n u_\alpha = 0 & \text{on } \Gamma. \end{cases} \quad (16)$

When $\alpha \to 0$, it is in some sense equivalent when v is regular to find the solution $u_N \in H^1(\Omega \setminus \gamma)$ to

$$\begin{cases} u_N = v & \text{in } \Omega \setminus \omega, \\ \Delta u_N = 0 & \text{in } \omega, \\ \partial_n u_N = \partial_n v & \text{on } \gamma, \end{cases} \quad (17)$$

which can be seen as a Neumann problem in ω.

From a numerical point of view, we will solve (16) with a very small positive α and we will consider that it is our Neumann problem. The Dirichlet problem does not require any special care.

The inpainting algorithm is then the following:

Inpainting algorithm

- Calculation of u_D and u_N, respectively solutions to

$$\begin{cases} u_D = v & \text{in } \Omega \setminus \omega, \\ \Delta u_D = 0 & \text{in } \omega, \\ u_D = v & \text{on } \gamma, \end{cases} \quad (18)$$

where $u_D \in H^1(\Omega)$, and

$$\begin{cases} -\alpha \Delta u_N + u_N = v & \text{in } \Omega \setminus \omega, \\ \Delta u_N = 0 & \text{in } \omega, \\ \partial_n u_N = 0 & \text{on } \Gamma, \end{cases} \quad (19)$$

where u_N is in $H^1(\Omega)$ (the normal derivative is the same on the two sides of γ).

- Calculation of p_D and p_N the two corresponding adjoint states, respectively solutions to

$$\begin{cases} p_D = 0 & \text{in } \Omega \setminus \omega, \\ -\Delta p_D = -(u_D - u_N) & \text{in } \omega, \\ p_D = 0 & \text{on } \gamma, \end{cases} \quad (20)$$
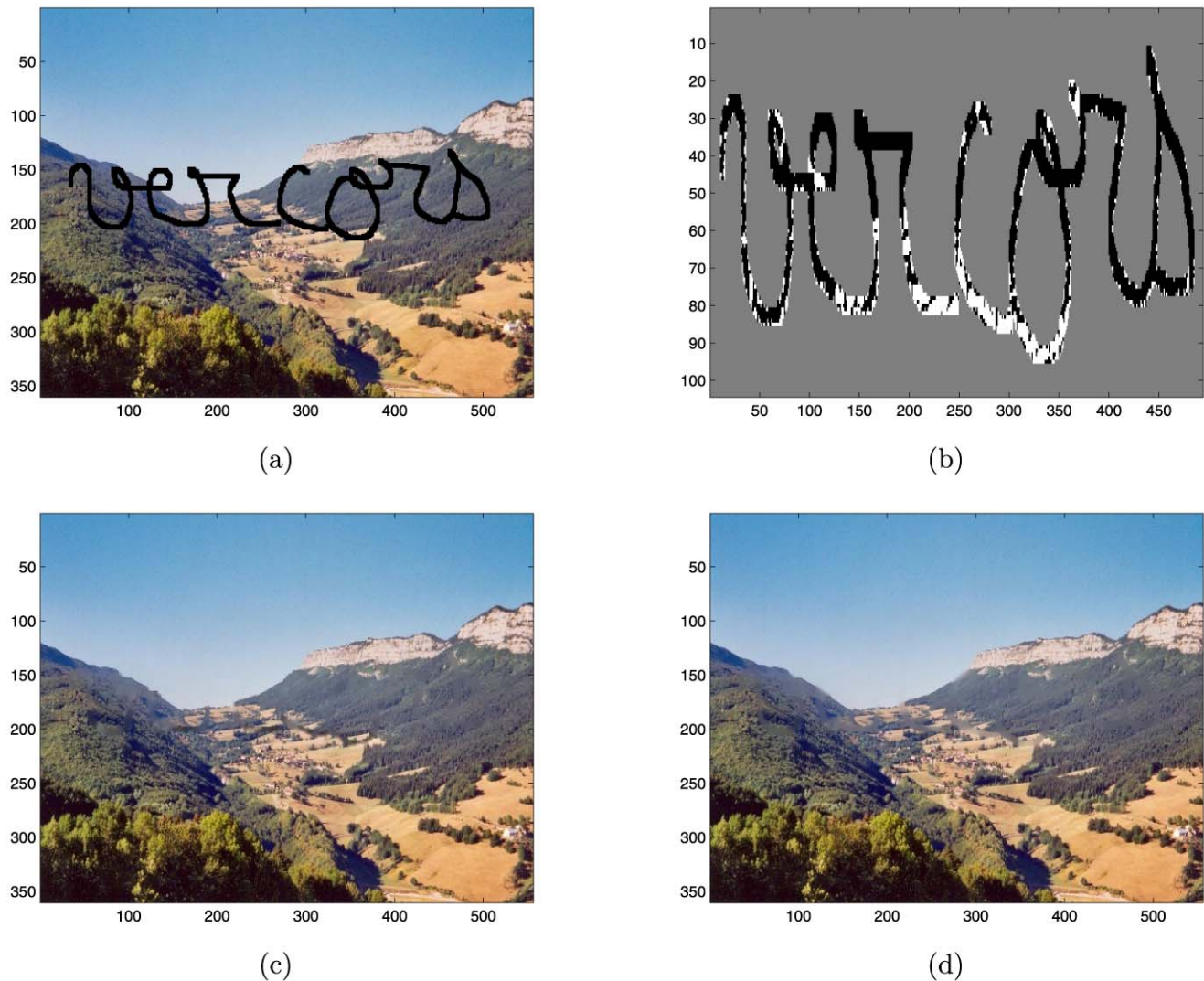
(a)

(b)

(c)

(d)

Fig. 2 Inpainting of a color image: occluded image (**a**); identified missing edges by the topological gradient (**b**); corresponding inpainted images using our algorithm (**c**) and a TV inpainting algorithm (**d**)

and

$$\begin{cases} p_N = 0 & \text{in } \Omega \setminus \omega, \\ -\Delta p_N = +(u_D - u_N) & \text{in } \omega, \\ \partial_n p_N = 0 & \text{on } \gamma. \end{cases} \quad (21)$$

- Computation of the 2×2 matrix $M(x)$ (see (14)) and its lowest eigenvalue λ_{min} at each point of the missing domain ω.
- Definition of cracks localization: $\{x \in \omega; \lambda_{min}(x) < \delta < 0\}$, where δ is a negative threshold.
- Calculation of u solution to the Neumann problem (7) taking into account the cracks location.

It is not so easy to take into account cracks, but from a numerical point of view, cracks are modeled by a small conductivity (see Sect. 4).

This algorithm has a complexity of $\mathcal{O}(n.\log(n))$, where n is the size of the image (i.e. number of pixels). See Sect. 6 for more details.

3.2 Numerical Results

We have applied our algorithm to the inpainting of a real color image.

Figure 2 shows respectively the occluded part by a black word (a), the identified missing edges (b) and the corresponding inpainted image by our algorithm (c). One can see that the reconstruction of the missing part of the image is very satisfactory, and all the occluded part has been treated at the same time. We also applied a TV inpainting algorithm (see e.g. [31] for details about this method) to the same image, and the result is shown in Fig. 2(d). For the TV inpaint-
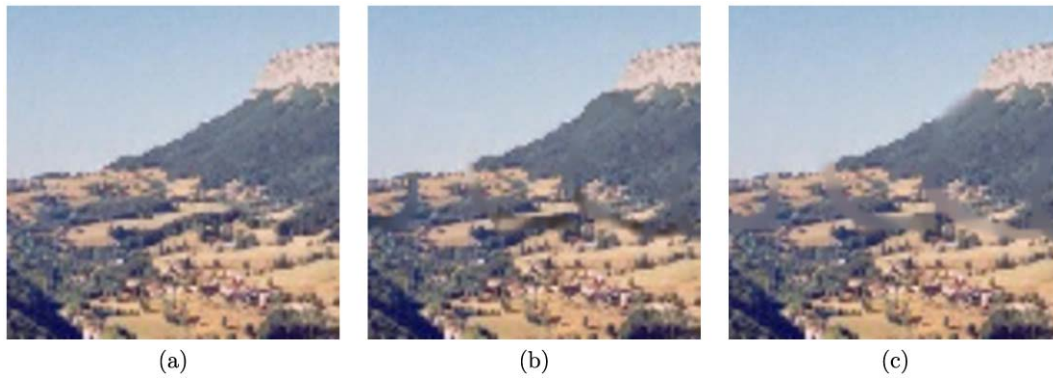
Fig. 3 Inpainting of a color image: zoom of original image (**a**); topological gradient inpainted image (**b**); TV inpainted image (**c**)

ing method we have used, the regularization coefficient is equal to 10^{-3}, and the lifting parameter is equal to 10^{-6}.

Figure 3 allows to compare more in details the original image (a) and the inpainted images using topological gradient (b) and total variation (c) algorithms. One can notice the remarkable sharp edges produced by our algorithm, as contrast to TV inpainting that slightly blurs edges.

There is no need to split the image into several parts, and the occluded part can have any geometry. It can even be a part of the image boundary, as our algorithm also works when the intersection of the inpainting domain and the boundary of the image is not empty. This comes from the fact that the crack localization algorithm can be very easily adapted to incomplete data on the boundary [14]. Moreover, the reconstruction is done in only one iteration of the topological gradient algorithm, which consists in 5 resolutions of a PDE (the two direct and two adjoint problems, and then one direct problem) in the domain Ω representing the image. Using a discrete cosine transform and a preconditioned conjugate gradient approach, it is possible to speed up these resolutions, and we obtain finally a $\mathcal{O}(n.\log(n))$ complexity (see Sect. 6 for more details).

4 Application to Image Restoration

In this section, we use the topological gradient as a tool for detecting edges for image restoration.

4.1 Variational Formulation and Topological Gradient

Let Ω be an open bounded domain of $\mathbb{R}^2$. For v a given function in $L^2(\Omega)$, the initial problem is defined in the safe domain and reads as follows: find $u \in H^1(\Omega)$ such that

$$\begin{cases} -\operatorname{div}(c\nabla u) + u = v & \text{in } \Omega, \\ \partial_n u = 0 & \text{on } \partial\Omega, \end{cases} \tag{22}$$

where n denotes the outward unit normal to $\partial\Omega$ and c is a constant function.

At a given point $x \in \Omega$, we insert a small crack $\sigma = \sigma(x, n, \rho)$, the new solution $u_\rho \in H^1(\Omega_\rho)$ satisfies

$$\begin{cases} -\operatorname{div}(c\nabla u_\rho) + u_\rho = v & \text{in } \Omega_\rho, \\ \partial_n u_\rho = 0 & \text{on } \partial\Omega_\rho. \end{cases} \tag{23}$$

Edge detection is equivalent to look for a subdomain of Ω where the energy is small. So our goal is to minimize the energy norm outside edges

$$j(\rho) = J_\rho(u_\rho) = \int_{\Omega_\rho} \|\nabla u_\rho\|^2. \tag{24}$$

By the mean of the topological asymptotic expansion theory, the variation of $j(\rho) = J_\rho(u_\rho)$ when ρ tends to zero is given by [15, 39, 40]:

$$j(\rho) - j(0) = f(\rho)g(x, n) + o(\rho^2), \tag{25}$$

with $f(\rho) = \pi\rho^2$,

$$g(x, n) = -c(\nabla u_0(x).n)(\nabla p_0(x).n) - |\nabla u_0(x).n|^2, \tag{26}$$

and where p_0 is the solution to the adjoint problem

$$\begin{cases} -\operatorname{div}(c\nabla p_0) + p_0 = -\partial_u J(u) & \text{in } \Omega, \\ \partial_n p_0 = 0 & \text{on } \partial\Omega. \end{cases} \tag{27}$$

The subscript 0 means that the solutions u_0 and p_0 are calculated in the initial domain without cracks; the crack size is equal to zero.

The topological gradient could be written as

$$g(x, n) = n^T M(x)n, \tag{28}$$

where $M(x)$ is the 2×2 symmetric matrix defined by

$$M(x) = -c\frac{\nabla u_0(x)\nabla p_0(x)^T + \nabla p_0(x)\nabla u_0(x)^T}{2} - \nabla u_0(x)\nabla u_0(x)^T. \tag{29}$$

For a given x, $g(x, n)$ takes its minimal value when n is the eigenvector associated to the lowest eigenvalue λ_{min} of M. This value will be considered as the topological gradient associated to the optimal orientation of the crack $\sigma(x, n, \rho)$.

4.2 Algorithm

Our algorithm consists in inserting small heterogeneities in regions where the topological gradient is smaller than a given threshold $\delta < 0$. These regions are the edges of the image. The algorithm is as follows

Restoration algorithm

- Initialization : $c = c_0$.
- Calculation of u_0 and p_0 : solutions of the direct (23) and adjoint (27) problems.
- Computation of the 2×2 matrix M and its lowest eigenvalue λ_{min} at each point of the domain.
- Set

$$c_1 = \begin{cases} \varepsilon & \text{if } x \in \Omega \quad \text{such that} \quad \lambda_{min} < \delta < 0, \quad \varepsilon > 0 \\ c_0 & \text{elsewhere.} \end{cases}$$
$$(30)$$

- Calculation of u_1 solution to problem (23) with $c = c_1$.

From the numerical point of view, it is more convenient to simulate the cracks by a small value of c. The solution u_1 is the restored image.

As in the previous section (inpainting problems), our algorithm requires only 3 resolutions of a partial differential equation in the domain Ω: the direct and adjoint original problems, and then the direct perturbed problem. And the complexity of this algorithm is still $\mathcal{O}(n.\log(n))$, where n is the number of pixels of the image, because we can use, as in the previous section, a DCT (discrete cosine transform) for the resolution of the first two problems, and then the DCT solver is used as a preconditioner to the PCG (preconditioned conjugate gradient) algorithm. See Sect. 6 for more details.

The restoration algorithm for color images is almost the same. For simplicity reasons, one can simply decompose the color image v in its channels: $v = (v^1, v^2, v^3)$ where v^i represents the intensity of the channel i. For instance, if we decompose the color image in the RGB (red, green, blue) space, v^1 will represent the intensity of red. Then, it is easy to solve equations (23) and (27) separately. But one can also solve directly this equation with vectorial images u and p. The topological gradient is still given by equalities (28) and (29), where all the involved functions are vectorial (it is simply the sum of these expressions for the three channels). One can finally solve separately the three perturbed direct problems, and recompose the restored image u_1, or solve directly the perturbed problem in a vectorial approach.

4.3 Numerical Results

The goal of the following numerical results is to prove that the topological gradient method is able to denoise an image and preserve features such as edges.

Figure 4 shows the restoration algorithm applied to a 556×360 color image. The noisy image (a) is obtained with an additive Gaussian noise, with a signal to noise ratio (SNR) equal to 10.74. The identified edges (b) correspond to the pixels where the most negative eigenvalue of the matrix M is smaller than a given threshold. The third image (c) corresponds to the restored image by our topological gradient algorithm. The SNR of the restored image is 21.09, and the edges are very well preserved, even if the original level of noise was quite high. Finally, the last image (d) shows the restored image via a Perona-Malik nonlinear diffusion model (see e.g. [11, 31]), using the following parameters: time $T = 2$, Gaussian filtering $\sigma = 10$ and threshold value equal to 15.

In order to see more clearly the noise reduction in this process, Fig. 5 shows the difference between the original and noisy images (i.e. the additive noise we added to the original image), and the error distribution after the restoration process (i.e. the difference between the original and restored images) for both the topological gradient and nonlinear diffusion schemes, using the same scale for the three images. One can see that the error is strongly reduced for both algorithms, with a slight advantage for our scheme. One can also notice that part of the topological gradient restoration error is still located on the contours, even if they are very well preserved by the process.

5 Application to Image Segmentation

This section is concerned with image segmentation, which aim is to find a partition of an image into its constituent parts.

Several variational approaches have been studied, for example the Mumford-Shah functional [45] and the active contours [23, 55].

5.1 Problem Setting

Let v be the original image defined on an open set Ω of $\mathbb{R}^2$. We want to split the image v in n classes $\{C_i\}_{1 \le i \le n}$, and we choose the color intensity as a classifier. The number of classes n is given.

More precisely, our goal is to find n colors C_i, $i = 1$, $\ldots, n$ and a partition of Ω in subsets $\{\Omega_i\}_{i=1,\ldots,n}$, such that v is close to C_i in Ω_i. The classified image u will then be defined by

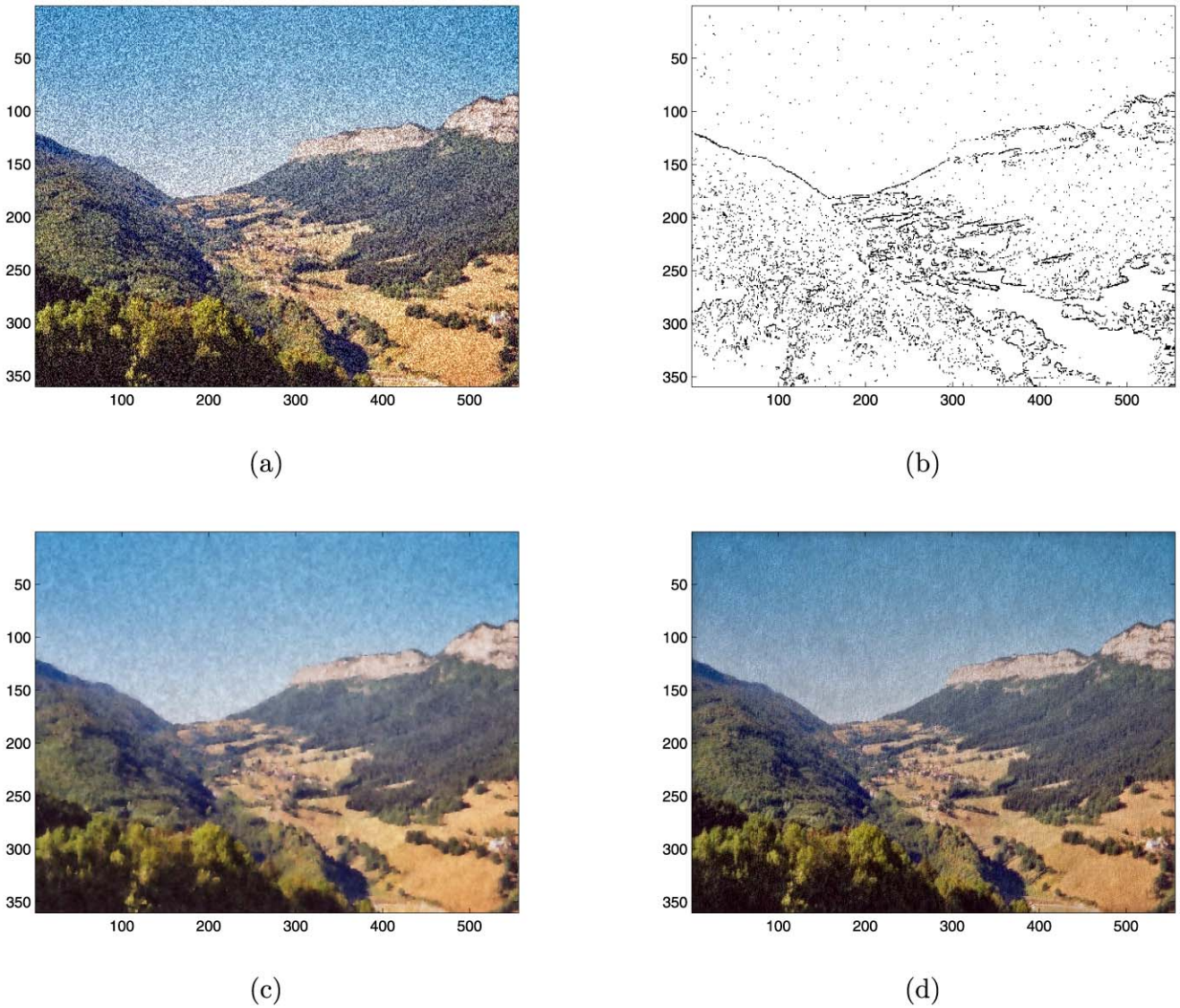$$u(x) = C_i \quad \forall x \in \Omega_i, \tag{31}$$

Fig. 4 Restoration of a color image: noisy image (SNR = 10.74, 556 × 360 pixels) (**a**); identified edges by the topological gradient (**b**); restored image using our restoration algorithm (SNR = 21.09) (**c**); restored image using Perona-Malik nonlinear diffusion (SNR = 19.87) (**d**)
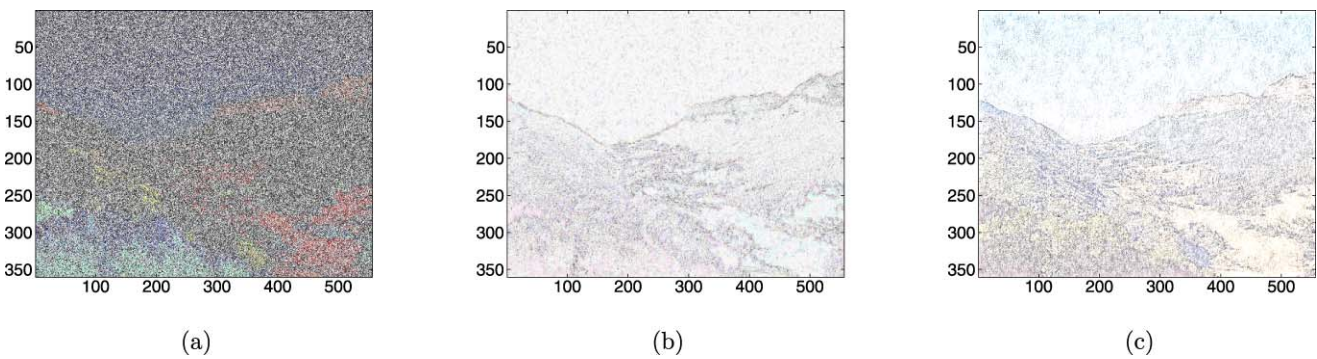

Fig. 5 Restoration of a color image: difference between the original and noisy images (**a**); difference between the original and restored images by topological gradient (**b**) and Perona-Malik nonlinear diffusion (**c**)

where $\{\Omega_i\}_{i=1,...,n}$ are defined by

$$\Omega_i = \{x \in \Omega; x \text{ belongs to the } i\text{th class}\}. \tag{32}$$

The variational approach consists in defining a cost function measuring the mean square difference between the original image and the segmented image

$$J\left((C_i, \Omega_i)_{i=1,...,n}\right) = \sum_{i=1}^{n} \int_{\Omega_i} (v(x) - C_i)^2 \, dx. \tag{33}$$

The minimization of J with respect to $(C_i, \Omega_i)_{i=1,...,n}$ could be done using the k-mean clustering algorithm. In order to obtain a segmented image with smoother contours (regularized segmentation), we may add a regularization term to the cost function

$$
\begin{aligned}
&J\left((C_i, \Omega_i)_{i=1,...,n}\right) \\
&= \sum_{i=1}^{n} \int_{\Omega_i} (v(x) - C_i)^2 \, dx + \sum_{i \neq j} |\Gamma_{ij}|,
\end{aligned} \tag{34}
$$

where $|\Gamma_{ij}|$, $i \neq j$ represents the one-dimensional Hausdorff measure of Γ_{ij} [11], and $\Gamma_{ij} = \Omega_i \cap \Omega_j$ is the interface between two subsets.

The main difficulty of this approach is that the unknowns are sets, and not variables. This is why the topological asymptotic analysis may be appropriate to solve this problem.

5.2 Restoration and Segmentation Coupling

Inspired by the work of Aubert et al. [11, 52] in which the authors propose a classification model coupled with a restoration process, we propose in this section to use the topological gradient approach applied to image segmentation problem [39].

We still consider the following partial differential equation

$$
\begin{cases}
-\operatorname{div}(c\nabla u) + u = v & \text{in } \Omega, \\
\partial_n u = 0 & \text{on } \partial\Omega.
\end{cases} \tag{35}
$$

Instead of setting $c = 0$ (or $c = \varepsilon$ from a numerical point of view) on the edge set and $c = c_0$ elsewhere, we set

$$
c = \begin{cases}
c = 0 \text{ (or } \varepsilon) & \text{on the edge set,} \\
c \sim +\infty \text{ (e.g. } c = \frac{c_0}{\varepsilon}) & \text{elsewhere.}
\end{cases} \tag{36}
$$

In comparison with the previous section, the topological gradient $g(x, n)$ and the general algorithm remains unchanged. In particular, the edge set is given by thresholding λ_{min}.

Segmentation algorithm

- Initialization: $c = c_0$.

- Calculation of u_0 and p_0 : solutions of the direct (23) and adjoint (27) problems.
- Computation of the 2×2 matrix M and its lowest eigenvalue λ_{min} at each point of the domain.
- Set

$$
c_1 = \begin{cases}
\varepsilon & \text{if } x \in \Omega \quad \text{such that} \quad \lambda_{min} < \delta < 0, \quad \varepsilon > 0 \\
c_0/\varepsilon & \text{elsewhere.}
\end{cases}
$$
$$\tag{37}$$

- Calculation of u_1 solution to problem (23) with $c = c_1$.
- Application of the k-mean classification algorithm to u_1.

From a numerical point of view, as ε is small on a contour, it allows u_1 to jump across edges with a normal derivative close to zero. Outside edges, $c = \frac{c_0}{\varepsilon}$ and then the PDE is nearly equivalent to $\Delta u = 0$ with Neumann boundary condition (normal derivative) equal to zero. The solution u_1 is then piecewise constant outside edges, providing a natural segmentation way of the image.

As in the restoration process, the segmentation algorithm is applied to color images. We simply decompose the image in a color space (RGB, or HSV), and deal separately with the three component images. Then we say the topological gradient of the sum is equal to the sum of topological gradients.

One can control the smoothing process in choosing the value of c outside the edges:

- if $c = c_0$, we find the previous restoration algorithm, which simply tries to remove noise;
- if $c = \frac{c_0}{\varepsilon}$, the smoothing is more powerful, and the final image is much smoother;
- if $c = \frac{c_0}{\varepsilon^2}$, it is much more powerful, and so on.

We can also mention that this is still the same type of algorithm, in comparison with the previous applications, and the complexity is still in $\mathcal{O}(n.\log(n))$, which allows us to classify quite large images in a short time.

In [16], the authors proposed an unsupervised classification method.

5.3 Numerical Results

We apply in this section our segmentation algorithm to synthetic monocolor grey images and to a real color one.

We first consider two different synthetic images, the first one consisting of 4 small squares of different grey levels, the second one consisting of 4 black different objects on a white background. We added a Gaussian noise to these images before trying to segment them, with a SNR equal to 18.2 and 17.1 respectively. Figure 6 shows the original images and the segmented images. In this case, we simply applied our segmentation algorithm. We can see on the first synthetic image that the four different components have been very well identified at the first iteration. It is also the same in the case of the
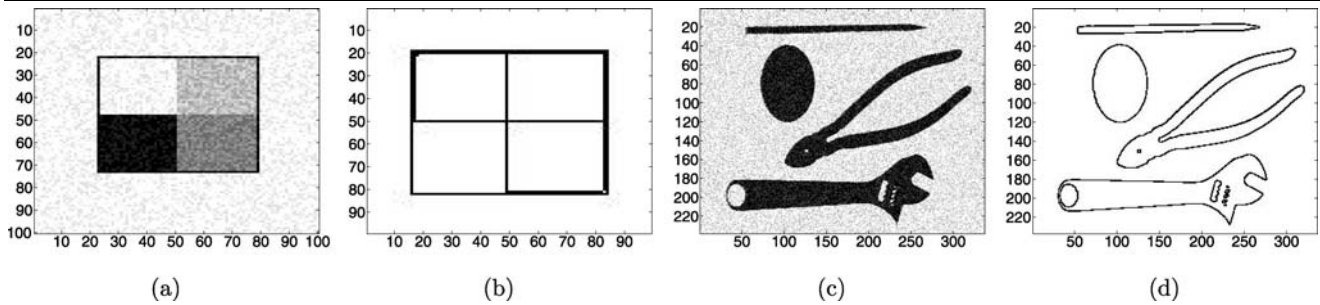
Fig. 6 Segmentation of synthetic images: noisy original images (SNR = 18.2 and 17.1 respectively) (**a–c**); segmented images (**b–d**)
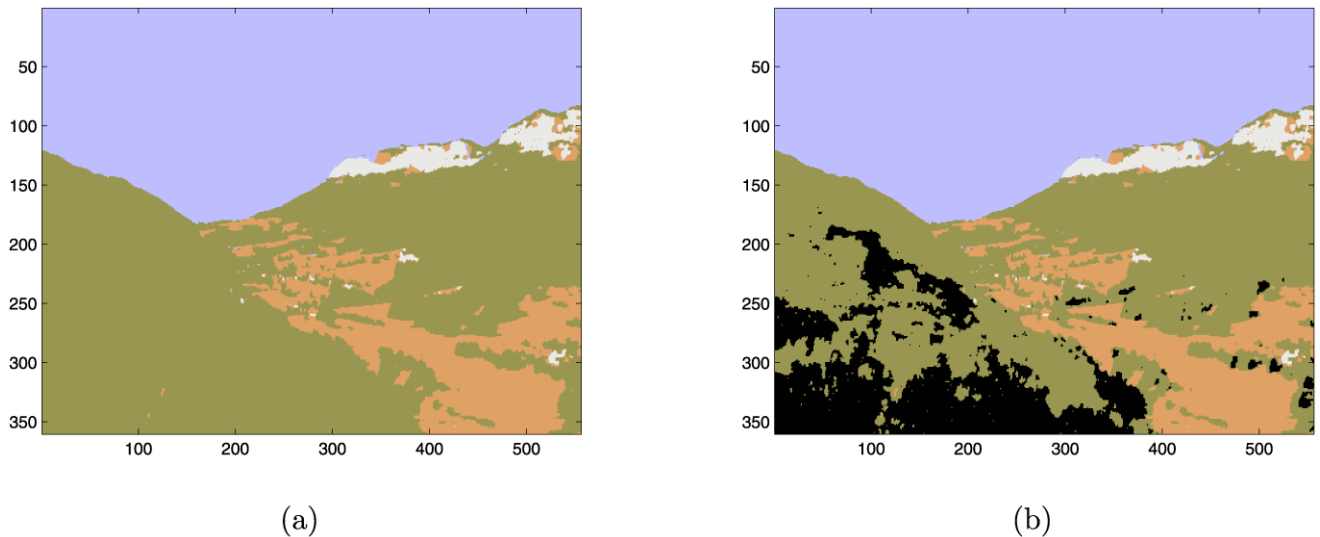

Fig. 7 Segmented images using respectively four (**a**) and five (**b**) colors

second synthetic image, the edges of all objects have been very well identified.

Figure 7 shows the application of our segmentation algorithm to a 556×360 color image (see previous figures, e.g. Fig. 2(c) for the original image). Figures 7(a) and 7(b) show respectively a 4 and 5 classes segmented image. One can see that there is a very good identification of the different components of the image (sky, forest, ground, ...).

6 Complexity and Speeding Up

In all the algorithms we presented, the first resolution of the PDE is done with a constant value of the coefficient. It is then possible to largely speed up the computation time by using the discrete cosine transform (DCT) method. Let us consider the following cosine basis (on $\mathbb{R}^2$, but it is easily adaptable to $\mathbb{R}^n$)

$$\phi_{m,n} = \delta_{m,n} \cos(m\pi x) \cos(n\pi y), \tag{38}$$

where we denote by x and y the two real variables, and $\delta_{m,n}$ are appropriate normalization coefficients. Then, the following PDE

$$\begin{cases} -\operatorname{div}(c\nabla u) + u = v & \text{in } \Omega, \\ \partial_n u = 0 & \text{on } \partial\Omega, \end{cases} \tag{39}$$
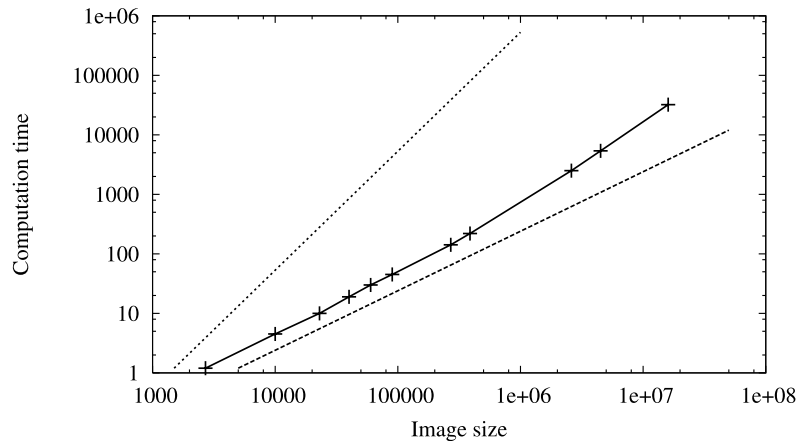
is equivalent to

$$\sum_{m,n} \left(1 + c(m\pi)^2 + c(n\pi)^2\right) u_{m,n}\phi_{m,n} = \sum_{m,n} v_{m,n}\phi_{m,n}, \tag{40}$$

where $(v_{m,n})$ represent the DCT coefficients of the original image v. It is then straightforward to identify $(u_{m,n})$, the DCT coefficients of u in (40), and then to compute u using an inverse DCT. The complexity of such a resolution is $\mathcal{O}(N \log(N))$, where N is the size of the image (i.e. the number of pixels).

This technique can be used for the resolution of both direct and adjoint equations. Then, for the last resolution of the

Fig. 8 Variation of the computation time according to the size of the image, using a log-log scale: linear and quadratic complexity in *dashed lines*, result of our experiments in *plain line*

direct problem with a non constant coefficient c, we have to solve the following system

$$A(c)u = B, \tag{41}$$

where u is the unknown image. We can precondition (41) with the DCT solver used in the first resolution. Equation (41) is equivalent to

$$A(c_0)^{-1}A(c)u = A(c_0)^{-1}B. \tag{42}$$

We use then a preconditioned conjugate gradient (PCG) method to solve this problem, and this works very well because in all our algorithms, the coefficient c is equal to c_0 except on a quite small part of the domain. For instance, in the restoration algorithm, $c = c_0$ except on the edges of the image.

Figure 8 shows the computation time versus the size of the image, using for both scales a logarithmic scale. The two dashed lines correspond to a linear and a square complexity. The middle curve corresponds to our various experiments. These experiments have been performed with the restoration algorithm, but all the other algorithms have the same behavior. This figure clearly confirms the theoretical complexity, $\mathcal{O}(N.\log(N))$, of our algorithms. For example, we have been able to restore without any trouble a few seconds of a large resolution movie on a laptop. The total number of pixels was greater than 16 millions.

7 Conclusion

We presented in this paper many applications in image processing of the crack detection technique, based on the topological gradient. It provides an excellent frame for solving all these image processing problems. It has been applied to image inpainting, image restoration, and image segmentation.

In all these cases, we obtained excellent results and the computing time is very short. Only $\mathcal{O}(n.\log(n))$ operations are needed to solve the image processing problem, where n is the size of the image.

We have also seen that this technique can be applied to color images as well as grey-level images, but also three-dimensional images, or movies, without any trouble.

One of our main goals is now to optimize our code in order to have a real time processing tool.

References

1. Alessandrini, G., Diaz Valenzuela, A.: Unique determination of multiple cracks by two measurements. SIAM J. Control Optim. **34**(3), 913–921 (1996)
2. Alessandrini, G., Beretta, E., Vessela, S.: Determining linear cracks by boundary measurements: Lipschitz stability. SIAM J. Math. Anal. **27**(2), 361–375 (1996)
3. Allaire, G.: Shape Optimization by the Homogenization Method. Applied Mathematical Sciences, vol. 146. Springer, New York (2002)
4. Allaire, G., Kohn, R.: Optimal design for minimum weight and compliance in plane stress using extremal microstructures. Eur. J. Mech. A Solids **12**, 839–878 (1993)
5. Allaire, G., Jouve, F., Taoder, A.M.: A level set method for shape optimization. C.R. Acad. Sci. Paris Ser. I **334**, 1125–1130 (2002)
6. Ammari, H., Vogelius, M.S., Volkov, D.: Asymptotic formulas for perturbations in the electromagnetic fields due to the presence of inhomogeneities of small diameter II—The full Maxwell equations. J. Math. Pures Appl. **80**(8), 769–814 (2001)
7. Amstutz, S., Masmoudi, M., Samet, B.: The topological asymptotic for the Helmoltz equation. SIAM J. Control Optim. **42**(5), 1523–1544 (2003)
8. Amstutz, S., Horchani, I., Masmoudi, M.: Crack detection by the topological gradient method. Control Cybern. **34**(1), 119–138 (2005)
9. Andrieux, S., Ben Abda, A.: Identification of planar cracks by complete overdetermined data: inversion formulae. Inverse Probl. **12**, 553–563 (1996)
10. Aubert, G., Aujol, J.-F.: Optimal partitions, regularized solutions, and application to image classification. Appl. Anal. **84**(1), 15–35 (2005)

11. Aubert, G., Kornprobst, P.: Mathematical Problems in Image Processing. Applied Mathematical Sciences, vol. 147. Springer, New York (2001)

12. Aubert, G., Vese, L.: A variational method in image recovery. SIAM J. Numer. Anal. **34**(5), 1948–1979 (1997)

13. Aujol, J.-F., Aubert, G., Blanc-Féraud, L.: Wavelet-based level set evolution for classification of textured images. IEEE Trans. Image Process. **12**(12), 1634–1641 (2003)

14. Auroux, D., Masmoudi, M.: A one-shot inpainting algorithm based on the topological asymptotic analysis. Comput. Appl. Math. **25**(2–3), 1–17 (2006)

15. Auroux, D., Masmoudi, M., Belaid, L.: Image restoration and classification by topological asymptotic expansion. In: Taroco, E., de Souza, E.A. (eds.) Variational Formulations in Mechanics: Theory and Applications. CIMNE, Barcelona (2006)

16. Auroux, D., Jaafar-Belaid, L., Masmoudi, M.: A topological asymptotic analysis for the regularized grey-level image classification problem. Math. Model. Numer. Anal. **41**(3), 607–625 (2007)

17. Belhachmi, Z., Bucur, D.: Stability and uniqueness for the crack identification problem. SIAM J. Control Optim. **46**(1), 253–273 (2007)

18. Ben Abda, A., Ben Ameur, H., Jaoua, M.: Identification of 2D cracks by elastic boundary measurements. Inverse Probl. **15**, 67–77 (1999)

19. Ben Abda, A., Kallel, M., Leblond, J., Marmorat, J.-P.: Line-segment cracks recovery from incomplete boundary data. Inverse Probl. **18**, 1057–1077 (2002)

20. Bendsoe, M.: Optimal topology design of continuum structure: an introduction. Technical Report, Department of Mathematics, Technical University of Denmark, Lyngby, Denmark (1996)

21. Bendsoe, M., Kikuchi, P.: Generating optimal topologies in structural design using an homogenisation method. Comput. Methods Appl. Mech. Eng. **71**, 197–224 (1988)

22. Berthod, M., Kato, Z., Yu, S., Zerubia, J.: Bayesian image classification using Markov random fields. Image Vis. Comput. **14**(4), 285–293 (1996)

23. Blake, A., Isard, M.: Active Contours. Springer, New York (1998)

24. Bouman, C.A., Shapiro, M.: A multiscale random field model for Bayesian image segmentation. IEEE Trans. Image Process. **3**, 162–177 (1994)

25. Bruhl, M., Hanke, M., Pidcock, M.: Crack detection using electrostatic measurements. Math. Model. Numer. Anal. **35**, 595–605 (2001)

26. Bryan, K., Vogelius, M.S.: A review of selected works on crack identification. In: Proceedings of the IMA Workshop on Geometric Methods in Inverse Problems and PDE Control, August 2001

27. Calderón, A.P.: On an inverse boundary value problem. In: Seminar on Numerical Analysis and Its Applications to Continuum Physics (Rio de Janeiro, 1980), Soc. Brasil. Mat., Rio de Janeiro, Brasil, pp. 65–73 (1980)

28. Catté, F., Coll, T., Lions, P.L., Morel, J.M.: Image selective smoothing and edge detection by non linear diffusion. SIAM J. Numer. Anal. **29**, 182–193 (1992)

29. Chan, T., Shen, J.: Mathematical models for local deterministic inpaintings. UCLA CAM Tech. Report 00-11, March (2000)

30. Chan, T., Shen, J.: Non-texture Inpainting by curvature-driven diffusions (CCD): UCLA CAM Tech. Report 00-35, September (2000)

31. Chan, T., Shen, J.: Image Processing and Analysis: Variational, PDE, Wavelet, and Stochastic Methods. SIAM, Philadelphia (2005)

32. Elad, M., Aharon, M.: Image denoising via sparse and redundant representations over learned dictionaries. IEEE Trans. Image Process. **15**(12), 3736–3745 (2006)

33. Elad, M., Starck, J.-L., Querre, P., Donoho, D.L.: Simultaneous cartoon and texture image inpainting using morphological component analysis (MCA). J. Appl. Comput. Harmon. Anal. **19**, 340–358 (2005)

34. Friedman, A., Vogelius, M.S.: Determining cracks by boundary measurements. Indiana Univ. Math. J. **38**(3), 527–556 (1989)

35. Friedman, A., Vogelius, M.S.: Identification of small inhomogeneities of extreme conductivity by boundary measurements: a theorem of continuous dependance. Arch. Ration. Mech. Anal. **105**(4), 299–326 (1989)

36. Garreau, S., Guillaume, P., Masmoudi, M.: The topological asymptotic for PDE systems: the elasticity case. SIAM J. Control Optim. **39**(6), 1756–1778 (2001)

37. Guillaume, P., Sididris, K.: The topological asymptotic expansion for the Dirichlet problem. SIAM J. Control Optim. **41**(4), 1042–1072 (2002)

38. Guillaume, P., Sididris, K.: The topological sensitivity and shape optimization for the Stokes equations. SIAM J. Control Optim. **43**(1), 1–31 (2004)

39. Jaafar Belaid, L., Jaoua, M., Masmoudi, M., Siala, L.: Image restoration and edge detection by topological asymptotic expansion. C.R. Acad. Sci. Sér. I **342**(55), 313–318 (2006)

40. Jaafar Belaid, L., Jaoua, M., Masmoudi, M., Siala, L.: Application of the topological gradient to image restoration and edge detection. Eng. Anal. Bound. Elem. **32**(11), 891–899 (2008)

41. Kohn, R., Vogelius, M.: Relaxation of a variational method for impedance computed tomography. Commun. Pure Appl. Math. **40**(6), 745–777 (1987)

42. Kubo, S., Ohji, K.: Inverse problems and the electric potential computed tomography method as one of their application. In: Mechanical Modeling of New Electromagnetic Materials. Elsevier, Amsterdam (1990)

43. Larrabide, I., Feijóo, R.A., Novotny, A.A., Taroco, E., Masmoudi, M.: An image segmentation method base on a discrete version of the topological derivative. In: Proc. 6th World Congress on Structural and Multidisciplinary Optimization, Brazil, June, 2005

44. Masmoudi, M.: The topological asymptotic. In: Glowinski, R., Karawada, H., Periaux, J. (eds.) Computational Methods for Control Applications, GAKUTO Internat. Ser. Math. Sci. Appl., vol. 16, Tokyo, Japan, pp. 53–72 (2001)

45. Mumford, D., Shah, J.: Optimal approximations by piecewise smooth functions and associated variational problems. Commun. Pure Appl. Math. **42**(5), 577–685 (1989)

46. Nishimura, N., Kobayashi, S.: A boundary integral equation method for an inverse problem related to crack detection. Int. J. Numer. Methods Eng. **32**, 1371–1387 (1991)

47. Paragios, N., Deriche, R.: Geodesic active regions and level set methods for supervised texture segmentation. Int. J. Comput. Vis. **46**(3), 223–247 (2002)

48. Pavlidis, T., Liow, Y.-T.: Integrating region growing and edge detection. IEEE Trans. Pattern Anal. Mach. Intell. **12**(3), 225–233 (1990)

49. Perona, P., Malik, J.: Scale space and Edge detection using Anisotropic diffusion. IEEE Trans. Pattern Anal. Mach. Intell. **12**, 629–639 (1990)

50. Samet, B., Amstutz, S., Masmoudi, M.: The topological asymptotic for the Helmholtz equation. SIAM J. Control Optim. **42**(5), 1523–1544 (2003)

51. Samson, C., Blanc-Féraud, L., Aubert, G., Zerubia, J.: A level set method for image classification. Int. J. Comput. Vis. **40**(3), 187–197 (2000)

52. Samson, C., Blanc-Féraud, L., Aubert, G., Zerubia, J.: A variational model for image classification and restauration. IEEE Trans. Pattern Anal. Mach. Intell. **22**(5), 460–472 (2000)

53. Santosa, F., Vogelius, M.: A computational algorithm to determine cracks from electrostatic boundary measurements. Int. J. Eng. Sci. **29**, 917–937 (1991)

54. Schumacher, A.: Topologieoptimisierung von Bauteilstrukturen unter Verwendung von Lopchpositionierungkrieterien. Ph.D. Thesis, Universitat-Gesamthochschule-Siegen, Germany (1995)
55. Sethian, J.A.: Level Set Methods and Fast Marching Methods: Evolving Interfaces in Computational Geometry, Fluid Mechanics, Computer Vision, and Materials Sciences. Cambridge Monograph on Applied and Computational Mathematics. Cambridge University Press, Cambridge (1999)
56. Sokolowski, J., Zochowski, A.: On the topological derivative in shape optimization. SIAM J. Control Optim. **37**, 1241–1272 (1999)
57. Sokolowski, J., Zochowski, A.: Topological derivatives of shape functionals for elasticity systems. Int. Ser. Numer. Math. **139**, 231–244 (2002)
58. Terzopoulos, D.: Regularization of inverse visual problems involving discontinuities. IEEE Trans. Pattern Anal. Mach. Intell. **PAMI-8**(4), 413–424 (1986)
59. Wang, M.Y., Wang, X.M., Guo, D.M.: A level set method for structural topology optimization. Comput. Methods Appl. Mech. Eng. **192**, 227–246 (2003)
60. Weickert, J.: Theoretical foundations of anisotropic diffusion in image processing. Computing **11**(Suppl.), 221–236 (1996)
61. Weickert, J.: Anisotropic diffusion in image processing. Ph.D. Thesis, University of Kaiserslautern, Germany (1996)
62. Weickert, J.: Efficient image segmentation using partial differential equations and morphology. Pattern Recognit. **34**(9), 1813–1824 (2001)
63. Wen, P., Wu, X., Wu, C.: An interactive image inpainting method based on RBF networks. In: Wang, J., et al. (eds.) LNCS, vol. 3972, pp. 629–637. Springer, Berlin (2006)
64. Zhou, T., Tang, F., Wang, J., Wang, Z., Peng, Q.: Digital image inpainting with radial basis functions. J. Image Graph. **9**(10), 1190–1196 (2004) (In Chinese)

Didier Auroux received his PhD in Applied Mathematics in 2003 from the University of Nice Sophia-Antipolis, France. Since 2004, he has been a faculty member of the Mathematics Institute of Toulouse, France, where he is currently an associate professor. He completed in 2008 his habilitation thesis. His research interests are in computational methods and their applications in data assimilation, image processing, and more generally optimal control and inverse problems.

Mohamed Masmoudi received the PhD degree in Applied Mathematics from the University of Nice Sophia-Antipolis (France), in 1979. He is currently Professor at the Mathematics Institute of Toulouse (France). He specializes in shape optimization methods and played a pioneering role in the development of the topological gradient. He is providing consulting in this field to leading companies of computer aided engineering. The topological gradient method seems to be particularly suitable for solving imaging and image processing problems.